NEUROSCIENCE

Hawkmoth lamina monopolar cells act as dynamic spatial filters to optimize vision at different light levels

Anna Lisa Stöckl[1,2]*, David Charles O'Carroll[1], Eric James Warrant[1]

How neural form and function are connected is a central question of neuroscience. One prominent functional hypothesis, from the beginnings of neuroanatomical study, states that laterally extending dendrites of insect lamina monopolar cells (LMCs) spatially integrate visual information. We provide the first direct functional evidence for this hypothesis using intracellular recordings from type II LMCs in the hawkmoth *Macroglossum stellatarum*. We show that their spatial receptive fields broaden with decreasing light intensities, thus trading spatial resolution for higher sensitivity. These dynamic changes in LMC spatial properties can be explained by the density and lateral extent of their dendritic arborizations. Our results thus provide the first physiological evidence for a century-old hypothesis, directly correlating physiological response properties with distinctive dendritic morphology.

INTRODUCTION

What neural form reveals about function has been a central question since the beginnings of neuroscience (*1*). One prominent functional hypothesis, dating back to Ramon y Cajal's work, is that laterally extending dendrites of insect lamina monopolar cells (LMCs) spatially integrate visual information (*2*). LMCs are the main relay neurons of the most distal neuropil of the insect visual system. The lamina is retinotopically organized into neural "cartridges"—one for each ommatidium of the compound eye—each of which contains the same set of neurons and processes one "pixel" of the image (Fig. 1). LMCs carry the visual information to the next optic neuropil, the medulla. They possess lateral dendrites, which, in many insect groups, extend into neighboring cartridges (*2*). In both Hymenoptera and Lepidoptera, it has been shown that the LMC dendrites of nocturnal species reach considerably more cartridges than those of diurnal species (*3*–*5*). On the basis of their distinctive morphology, it has long been suggested that LMCs perform spatial processing via their lateral dendrites [Fig. 1, B and C; reviewed in (*6*)]. This would allow LMCs to dynamically optimize visual perception over a wide range of light levels (*7*, *8*). However, direct functional evidence for this hypothesis is lacking.

Electrophysiological data from dipteran flies showed that the responses of LMCs contain signatures of lateral inhibition at bright light intensities and spatial summation in dim light (*9*–*11*). However, Diptera constitute an exception among insects because the dendrites of their major LMC types do not extend beyond their "home" cartridge (*12*, *13*). Thus, while in fly LMCs spatial integration was demonstrated functionally, the morphology of these cells does not support it. It was therefore suggested that spatial summation is generated through electrical coupling of photoreceptors within one fly ommatidium (*9*, *10*). Because higher Diptera possess neural superposition compound eyes and open rhabdoms, the photoreceptors within a single ommatidium each receive information from different neighboring points in the visual scene (*14*, *15*). Thus, pooling photoreceptor responses from a single ommatidium would result in spatial summation.

This form of spatial integration is, however, not possible in most other insect groups where photoreceptors within each ommatidium form a fused rhabdom and share a single optical axis. Because the absence of neural superposition widely coincides with LMCs featuring prominently extending dendrites, the hypothesis remains that insects other than Diptera use their extensive LMC dendrites for spatial integration. To test this hypothesis, we physiologically quantified the spatial properties of LMCs in the hawkmoth *Macroglossum stellatarum*, which exhibits spatial summation in its motion vision system in dim light (*16*) and features LMCs with dendrites extending beyond their home cartridge (*5*). Our results not only confirm this hypothesis but also show that the morphology of LMCs is intimately connected to their function by dynamically shaping spatial information processing to optimize vision at different light levels.

RESULTS

We characterized the responses of type II LMCs (*5*) because this LMC type possesses dendrites that extend into neighboring cartridges, and is unequivocally identifiable by its dendritic morphology (fig. S4). To obtain their spatial response profile, we stimulated them with a moving narrow black bar on a white screen while intracellularly recording their responses. When the black bar entered an LMC's receptive field, it responded to this brightness decrement with an increase in membrane potential (Fig. 2), as opposed to photoreceptors, which responded in a sign-conserving manner (see also fig. S2 for responses to full-field brightness increments and decrements). We

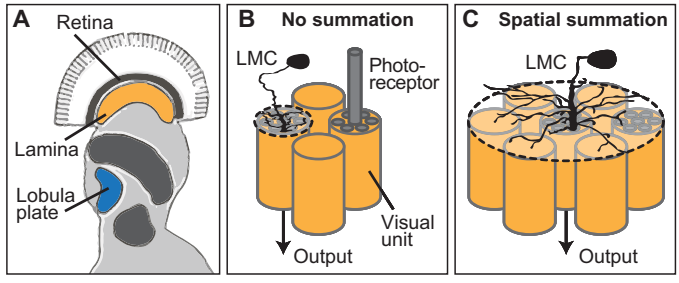

Fig. 1. Spatial summation in the insect lamina. (**A**) Spatial integration of visual information in insects is thought to occur in the lamina (orange), the first visual processing area of their brain. (**B**) Its main relay neurons, LMCs, receive visual information from the axons of photoreceptors. (**C**) LMCs in many insect species possess laterally extending dendrites, which reach into neighboring visual units processing neighboring "pixels" of the image. By pooling information from their lateral dendrites LMCs could thus perform spatial summation.

[1]Department of Biology, Lund University, Lund, Sweden. [2]Department of Behavioral Physiology and Sociobiology, Würzburg University, Würzburg, Germany.
*Corresponding author. Email: anna.stoeckl@uni-wuerzburg.de

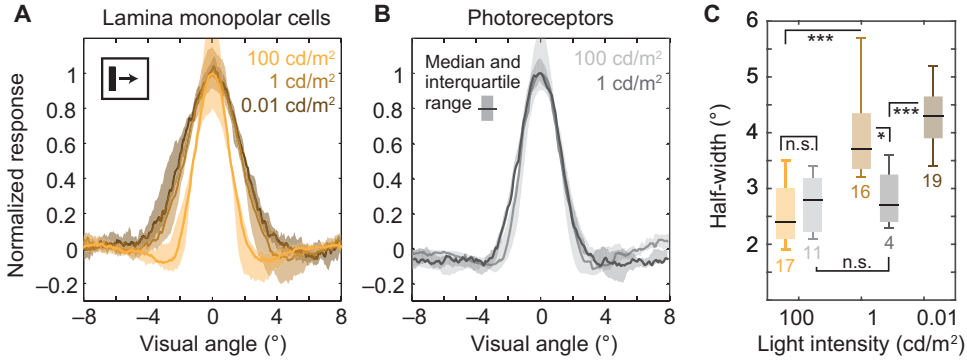

Fig. 2. Responses of LMCs at lower light intensities show evidence of spatial summation. The spatial response properties of LMCs (**A**) and photoreceptors (**B**) were probed with a moving bar at three light intensities (100, 1, and 0.01 cd/m^2). The photoreceptor responses are sign-inverted for comparability, and all responses are normalized by the integral of each individual response. Because photoreceptors only responded with isolated photon bumps at 0.01 cd/m^2, we did not obtain a spatial response curve. Solid lines represent medians, and the shaded areas represent the interquartile ranges. (**C**) Spatial tuning changed only in LMCs, as shown by receptive field half-widths [numbers below the boxes indicate number of recordings; analysis of variance (ANOVA) with Bonferroni-corrected post hoc test; table S1]. n.s., not significant. *P < 0.05, **P < 0.01, ***P < 0.001.

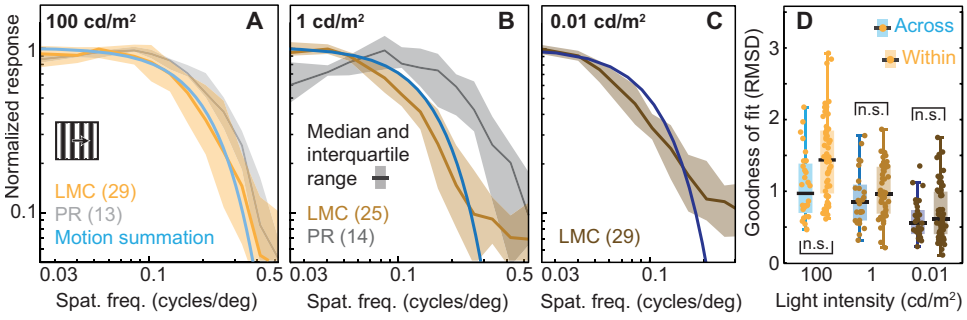

Fig. 3. Responses of LMCs explain spatial summation in wide-field motion neurons. (**A** to **C**) We measured the spatial responses of LMCs (brown hues) and photoreceptors (PR) (gray hues) using the same sinusoidal moving gratings that were previously used for downstream lobula plate motion-sensitive neurons (*16*). LMC responses were quantified as the power in the voltage trace at the temporal frequency of the grating. Solid lines represent medians, and the shaded areas represent the interquartile ranges. Numbers of recordings are shown in brackets. Norm., normalized; Spat freq, spatial frequency. (**D**) The LMC responses were compared to the spatial summation predicted from the motion neuron's response [in the form of a Gaussian spatial summation filter convolved with the photoreceptor spatial response at each light intensity (blue lines); (*17*)]: We quantified the goodness of fit using the root mean square deviation (RMSD) between the summation kernel and lamina responses (across) and compared it to deviations within the lamina cell responses (within) at each light intensity. The spatial summation kernel's deviation was either significantly smaller or not significantly different from that within the LMC responses, suggesting a good fit (ANOVA with Bonferroni-corrected post hoc test; table S2 and fig. S5).

recorded hawkmoth LMC spatial receptive fields in response to the moving bar at a range of average screen intensities (100, 1, and 0.01 cd/m^2) to test whether indications of spatial summation appeared with decreasing light intensity, as observed in Dipteran LMCs (*10*, *11*). In bright light, LMC spatial receptive fields were narrow and had mild lateral inhibitory flanks, adaptations favoring enhanced spatial resolution. As light levels decreased 100-fold, the lateral inhibitory flanks disappeared, and a significant broadening of the LMC spatial receptive field occurred, as quantified by the full width at half maximum, termed "half-width" henceforth, which indicates spatial summation (Fig. 2, A and C). This broadening could not be explained by changes in the earlier processing stage, as the photoreceptors showed no significant increase in spatial receptive field width (Fig. 2, B and C). Moreover, at the lowest light intensity tested, photoreceptors—unlike LMCs—failed to respond with distinct membrane potential variations [and instead only responded with isolated photon bumps, as previously reported; (*16*)], demonstrating that a significant increase in sensitivity took place downstream of the photoreceptors. We therefore conclude that the spatial summation observed in the responses of LMCs, which widens their receptive fields and improves their visual sensitivity, likely originates within the lamina.

Spatial summation has previously been described in hawkmoths, but it was quantified indirectly from the responses of wide-field motion-sensitive neurons (*16*, *17*). Assuming a general homology of the motion vision pathway of hawkmoths with the well-described pathway in Diptera (*18*–*20*), the motion-sensitive neurons in the lobula complex (Fig. 1A) are at least four synapses downstream of the photoreceptors, leaving many possible candidate neurons as the source of spatial summation in the lamina and medulla (*19*–*23*). The extent of spatial summation was extracted from these motion responses by comparing their spatial tuning to that of photoreceptors using a physiologically tuned motion correlator model with a spatial summation term (*16*). We tested whether the spatial tuning of LMCs can explain the spatial dynamics of the wide-field motion vision neurons and thus whether LMCs could be the source of the spatial summation observed. By comparing the spatial summation kernels previously quantified from the motion vision system (Fig. 3, A to C, blue lines; see Materials and Methods for details) to the spatial properties of LMCs (tested with the same moving gratings as the motion neurons—Fig. 3, A to C, brown hues), we found that the summation kernels fitted the LMC responses at each corresponding light intensity very well [goodness of fit was evaluated as root mean

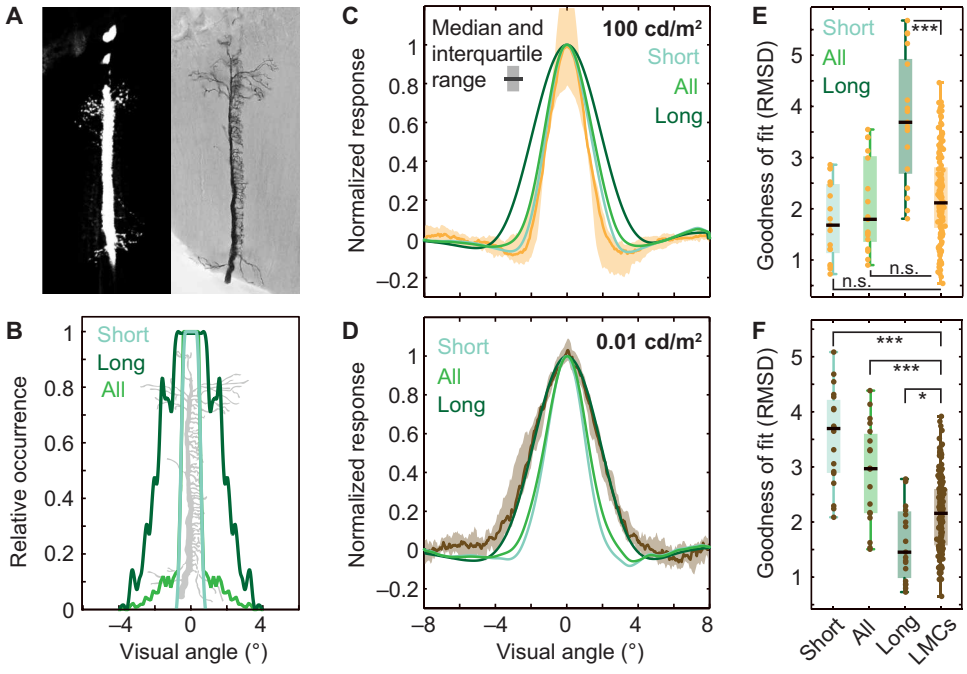

Fig. 4. Dendritic morphologies of LMCs are matched to physiological responses. (**A**) By injecting neurobiotin into a subset of recorded LMCs, we characterized these cells as type II LMCs (see also figs. S2 and S3) (*5*). (**B**) For this LMC type, we constructed spatial filters based on the dendrite histogram of these cells, including all dendrites (green), only the long dendrites (dark green), or only the short core dendrites (light green). (**C** and **D**) By convolving these dendritic filters with the spatial receptive fields of the photoreceptors at each light intensity, we predicted the spatial responses of the LMCs given integration of photoreceptor responses from these dendrites. (**E** and **F**) We tested the goodness of fit between these predicted responses and the physiological data by calculating their RMSD (short, all, and long). These were compared to the RMSD within LMC responses (LMCs). Significantly smaller or nonsignificant deviations between models and the LMC population indicate good fits, while significantly larger deviations do not (ANOVA with Bonferroni-corrected post hoc test; table S3). *$P < 0.05$, **$P < 0.01$, ***$P < 0.001$.

square deviation (RMSD); Fig. 3D]. This was not the case for summation kernels compared to LMC responses at different light intensities (fig. S5), highlighting that these fits were very specific. Because the LMC responses entirely explained the previously observed spatial summation in the wide-field motion neurons of *M. stellatarum* and because the upstream photoreceptors did not show corresponding changes in spatial tuning (Figs. 2B and 3B), we conclude that LMCs are very likely the cells responsible for spatial summation in hawkmoth motion vision.

Lastly, we tested whether the spatial summation we observed in LMCs can be explained by their specific dendritic morphology by characterizing the morphology of a subset of the recorded LMCs via neurobiotin injections. All injected neurons were identified as type II LMCs (Fig. 4A and fig. S3). We confirmed that there was no significant difference in the spatial responses of identified and unidentified LMCs (fig. S3), suggesting that all recorded neurons were type II LMCs or indistinguishable by their physiological responses. Having established the identity of the neurons, we used a previously established morphological characterization of LMC types (*5*) to generate spatial filters predicting LMC responses based on dendritic integration (Fig. 4B; see Materials and Methods for details). Because type II LMCs have two distinct dendritic populations—one population of shorter, branched dendrites remaining in the home cartridge (Fig. 4B, bright green) and one population of longer, "smoother" dendrites extending into neighboring cartridges (Fig. 4B, dark green)—we generated response predictions for those two populations and for integration from all dendrites (green). These predictions were compared to actual LMC responses at the brightest and dimmest light intensity to evaluate whether the spatial properties of LMCs were generated by spatial integration from specific subsets of dendrites.

At the brightest light intensity, integration from the short dendrites fitted the LMC responses significantly better than the other dendrite models (goodness of fit was quantified as RMSD smaller or equal to the deviation within LMC responses; Fig. 4, C and E). At the dimmest light intensity, the opposite was true: Integration exclusively from the long dendrites best fitted the responses (Fig. 4, D and F). We therefore conclude that the spatial response properties of type II LMCs can be fully explained by their dendritic morphology. Moreover, we can explain the dynamic changes seen in the spatial properties of LMCs at different light levels by a differential integration of the two subsets of dendrites.

DISCUSSION

Our study provides the first definitive connection between the well-described dendritic morphology of insect LMCs and their long-hypothesized function in spatial integration. We show that hawkmoth LMCs feature high spatial resolution in bright light in response to a moving bar but enhance visual sensitivity in dim light by spatially summing visual information, thereby acting as dynamic spatial filters. Crucially, we demonstrate that this spatial filtering can be quantitatively explained by integration of photoreceptor signals at the LMC's lateral dendrites, with integration switching between shorter and longer dendrites depending on light intensity.

These findings raise a number of intriguing new questions. First, how is this dynamic change in synaptic weighting between longer

and shorter dendrites implemented at a cellular level? Anatomical work in the butterfly *Papilio aegis* shows that both the long and short dendrites of lamina monopolar cell type (L2), which closely resemble our type 2 LMCs in dendritic morphology, have postsynaptic connections with photoreceptor terminals, both in their own and in neighboring cartridges, suggesting that this type of LMC is likely to have the connectivity required for the spatial summation observed in this study. However, to explain the dynamic change in their spatial properties, a gating mechanism would be necessary to suppress the synaptic connections of the long dendrites in bright light or disinhibit them in dim light. A lamina interneuron, or a medulla neuron projecting to the lamina, might carry information on average light intensity or adaptation state and provide this gating feedback to the system, consistent with their hypothesized role in providing adaptation, gain control, or behavioral state modulation to the lamina (*24*). Moreover, the long dendrites of this LMC type in *P. aegis* also form synaptic connections onto each other (*25*). These connections between neighboring type II LMCs could be a straightforward way to provide lateral inhibition to the system. Again, these synapses might only be active in bright light and might even be suppressed by the same mechanism that activates (or disinhibits) the synaptic connections to the photoreceptors on these dendrites—just with opposing polarity. It remains to be determined whether these lateral connections exist in the type II LMCs of *M. stellatarum*.

In this study, we have focused our investigation on type II LMCs. However, *M. stellatarum*, like all other insects, has a number of distinct LMC types, which repeat in every cartridge (*6*) and differ in their dendrite morphology (*5*). Expanding our findings to these other LMC types suggests that their specific dendritic profiles should result in different spatial response properties, creating a number of parallel spatial channels that process each "pixel" of visual information. The idea of segregating visual information into different parallel feature channels via different LMC types is in line with recent findings that different LMC types in flies and butterflies differ in their temporal response properties (*26*, *27*), and those in bumble bees and *Drosophila* have different luminance, polarity, and contrast coding properties (*28*, *29*).

Our results also quantitatively match the spatial summation previously observed in the hawkmoth motion vision system, thus giving the strongest evidence to date that the spatial summation previously described in wide-field motion vision neurons of hawkmoths (*16*, *17*) has its origin in the lamina. This also agrees with theoretical considerations and computational modeling, suggesting that spatial summation for the purpose of noise reduction should occur as early as possible in the visual system to be most effective (*17*, *30*). This does not rule out the possibility that other integrating neurons interact with the motion vision pathway in the lamina (*24*), and especially in the medulla (*19*, *20*), to influence the spatial tuning of this pathway, but our results suggest that general spatial tuning, with its improvements in signal-to-noise ratio at dimmer intensities, is generated in the lamina. However, the wide receptive fields of these integrating neurons might also serve other purposes, such as a general gain adjustment, or the tuning of directional responses (*31*), and thus, physiological recordings will be instrumental to understand their role in the motion processing pathway.

Lastly, our findings in hawkmoths provide an alternative model of spatial integration in the early visual system of insects to that based on findings in *Drosophila* (potentially representative for dipteran flies): While electrophysiological data from dipteran LMCs show lateral inhibition in bright light and spatial summation in dim light (*9*–*11*), they do not possess dendrites extending beyond their home cartridge (*12*, *13*). Thus, there is no anatomical basis for lateral integration based on direct dendritic input to the LMCs—with the exception of L4, which has, so far, not been shown to play a role in shaping the spatial tuning of its visual outputs (*24*). An alternative mechanism for spatial summation in the early visual system of Diptera was therefore suggested, one based on their unique eye type—the neural superposition compound eye. The photoreceptors within each fly ommatidium receive information from different neighboring points in the visual scene (*14*, *15*). Thus, electrically coupling photoreceptors within one fly ommatidium can result in spatial summation (*9*, *10*). It remains to be shown how lateral inhibition is generated in the flies where it has been observed (*9*–*11*). A simple mechanism based on direct interactions between L2 neurons—as is anatomically possible in butterflies and moths—is not possible in *Drosophila*, as these connections do not exist (*21*). Given these differences between hawkmoth LMCs and those of flies and given the similarities of hawkmoths to many other insect groups also featuring LMCs with laterally extending dendrites, it is likely that early visual processing—particularly in the spatial domain—differs between the Diptera and many other insect groups. Future comparative research on a variety of insect groups can shed light on these exciting questions and distinctly expand our understanding of spatial processing in insect vision.

MATERIALS AND METHODS

Animals

Adults of *M. stellatarum* were cultured from eggs obtained from wild-caught adult individuals collected in France (Sorede) and fed on their native host plants *Galium* sp. Adult moths (male and female) were kept in flight cages on a 14-hour day/10-hour night light regime and fed with a 10% sugar solution for at least 2 days before being used for experiments.

LMC recordings

Moths were restrained by cutting off their wings and taping the thorax tightly to prevent movement of the flight muscles. The head and thorax were fixed to the tape and to each other with wax to prevent movements. A small hole was cut into the head capsule to the right of the dorsal margin of the left compound eye, above the proximal rim of the lamina. The lamina was exposed by removing the overlaying air sacs and the brain membrane. An indifferent electrode of thin silver wire was inserted through a second hole made in either the other eye or elsewhere on the head capsule. A glass microelectrode (borosilicate glass, filled with 2 M potassium chloride, 120 to 200 megaohm in vivo) was inserted through the hole and advanced into the lamina using a Märzhäuser piezo-driven manipulator. Intracellular penetrations of LMCs were identified by resting potentials between −40 and −60 mV and distinguished from photoreceptor responses by hyperpolarizing responses to flashes of light (figs. S1A and S2). Neural responses were amplified 10 times for intracellular recordings (BA-03X, NPI Electronics, Tamm, Germany) and monitored with an oscilloscope and an audio monitor. Signals were digitized at a sampling rate of 5 kHz using a data acquisition card (USB 6221, National Instruments) and stored on a personal computer using custom software written in MATLAB (R2010a, The MathWorks, Natick, MA).

Electrode tips were filled with 4% neurobiotin (Vector Laboratories, Burlingame, USA) in a 1 M KCl solution and were backfilled with 1 M KCl. After recordings, neurobiotin was iontophoretically injected into the neurons using a constant depolarizing current of 2.5 nA for between 30 s and 5 min.

Photoreceptor recordings

Photoreceptor recordings were reanalyzed from (*16*). In brief, moths were restrained as for LMC recordings. A small hole (10 to 15 facets wide) was cut near the dorsal margin of the left compound eye. The hole was sealed with Vaseline to prevent it drying out. An indifferent electrode of thin silver wire was inserted in the other eye. A glass microelectrode (borosilicate glass, filled with 2 M potassium chloride, 150 to 200 megaohm in vivo) was used for recordings. Intracellular penetrations of photoreceptors were distinguished by resting potentials between −40 and −60 mV and depolarizing responses to flashes of light (figs. S1A and S2). Neural responses were amplified, digitized, and stored as described above for LMC recordings.

Histology

Brains containing neurobiotin-injected neurons were prepared as described previously (*17*). In short, the dissected brains were fixed in neurobiotin fixative at 4°C overnight. Brains were then washed and incubated with streptavidin conjugated to Cy3 (Dianova, Hamburg, Germany) 1:1000 for 3 days at 4°C. After incubation, brains were rinsed and then dehydrated in an ascending ethanol series and then cleared with methyl salicylate. The brains were lastly embedded as whole-mount preparations in Permount (Fisher Scientific, Pittsburgh, PA).

Whole-mount preparations ($n = 22$) were scanned with a confocal laser scanning microscope (SP8, Leica) using a 20× oil immersion objective (HC PL APO CS2/0.75, Leica) and a white light laser. The resolution of image stacks was 1024 × 1024. For presentation, a maximum intensity projection of the confocal image stack containing an LMC was generated using FIJI (fig. S4) (*32*).

Stimulation

Stimulus presentation and calibration were applied with the same equipment as previously described (*16*, *17*). Stimuli were presented on a liquid crystal display (SyncMaster 2233SW, Samsung) with a mean luminance of 100 cd/m^2 (equivalent to early dusk light levels) at a frame rate of 120 Hz. Stimuli were generated and controlled by custom software written for Psychtoolbox (version 3.08, 2010; www.psychtoolbox.org) running under MATLAB 2008b on a Macintosh computer with an Nvidia Quadro graphics processing unit. The screen was positioned 37 cm in front of the animal, permitting production of patterns subtending approximately 70°. The intensity of the display could be reduced in 0.5 $\log_{10}$ unit steps using large custom-made neutral density filters (Melles Griot). A matte black spray-painted metal cone (i.e., a black stiff-walled bellows with four sides) was attached over the screen. The filters were mounted on the narrow opening at the frontal end of this cone to attenuate light emitted from the screen. The moth was adjusted to face the front filter and thereby view the attenuated screen. The screen could be moved radially around the animal during experiments to position the center of the screen in the center of the receptive field of the recorded cell.

Data were obtained at three light intensities: 100, 1, and 0.01 cd/m^2. The animal was adapted to a blank screen at each light intensity for 30 min. Because we rarely recorded from single LMCs for longer than 30 min, different neurons were recorded at the different light intensities. Each trial consisted of a prestimulus time (minimum, 1 s) when the cell was exposed to a blank screen with the mean intensity of the stimulus trial, followed by the stimulus, which, in turn, was followed by a poststimulus rest period of 1 s, again displaying the blank screen. Two types of stimuli were used to characterize the spatial response features of the cells: a moving black bar on a white background (maximum contrast) and horizontally drifting sinusoidal gratings [to directly compare the lamina neuron's spatial responses with those previously described for motion-sensitive neurons; (*17*)]. Before measuring spatial responses, we used a brief (less than 8 ms) incremental flash of the entire screen to measure neuronal impulse responses to determine whether we were recording from an LMC (voltage decrement response to a brightness increase) or a photoreceptor (voltage increment to brightness increase; see fig. S2).

The moving black bar had an angular extent of 2.5° and moved at 22°/s, the same stimulus previously used for the photoreceptor recordings (*16*, *17*). The sinusoidal black and white gratings were moved at a temporal frequency of 2 Hz for photoreceptors and 4 Hz for LMCs and had spatial frequencies of 0.026, 0.041, 0.054, 0.084, 0.105, 0.133, 0.166, 0.209, 0.263, 0.332, 0.418, and 0.525 cycles/deg, respectively. In response to the moving grating, the graded potential responses of LMCs rose and fell as the dark and bright bars of the grating passed through their receptive field. We defined the response amplitude to these gratings as the amplitude of the power at the given temporal frequency in the Fourier transform of the neurons' oscillating response waveform.

Data analysis

Data were analyzed using MATLAB (The MathWorks, Nattick, MA). A total of 107 LMCs were recorded, from which 52 receptive fields were measured with the moving bar stimulus (17 at 100 cd/m^2, 16 at 1 cd/m^2, and 19 at 0.01 cd/m^2) and 83 responses to moving sinusoidal gratings (29 at 100 cd/m^2, 25 at 1 cd/m^2, and 29 at 0.01 cd/m^2).

Averages of the LMC and photoreceptor responses to moving bars (Fig. 2) were generated by normalizing each response by its cumulative sum before averaging to preserve the shape of the responses and then normalizing the average to 1. To account for the impact of the stimulus on the measured receptive field size, we "deconvolved" the stimulus shape from the recorded neuron's receptive field (fig. S1B) using a similar approach as developed in earlier work (*33*) and described in detail as applied here in (*34*). In brief, we fitted the neuron's responses to a model comprising a convolution of a Gaussian acceptance function, where the free parameter to fit was the full width at half maximum, termed half-width henceforth, of the Gaussian and a square wave function with the width of the bar stimulus. This convolution result was then fitted to the photoreceptor and LMC responses to obtain a model of the (Gaussian) receptive field given the particular stimulus applied. The half-width of the Gaussian model obtained from the fit was used for further analysis, where we compared the half-widths of LMC responses with those of the photoreceptors across light intensities using an analysis of variance (ANOVA) with a Bonferroni-corrected post hoc test (table S1). Normality of the test residuals was confirmed using a Lilliefors test. We noted that the photoreceptor receptive field half-widths obtained with this method from the bar stimulation experiments did slightly exceed those obtained with a different method in a previous study (*16*). The receptive field half-widths

in this study were obtained using moving sinusoidal gratings to use the same stimuli as for the wide-field motion neurons studied in this project. Fourier-transformed Gaussian functions were fitted to the responses to extract a receptive field half-width estimate. The difference in stimulation might be the reason for the different receptive field half-width estimates, suggesting that the photoreceptors did not respond linearly to different types of stimuli. This is in line with previous observations of their temporal response properties with different stimuli [discussed in (*17*)].

To quantify an LMC response to sinusoidal gratings (fig. S1C), we extracted the power of its oscillating response waveform at the stimulus' temporal frequency of 2 Hz in the Fourier spectrum (Fig. 3, A to C). To determine whether these spatial responses could explain the spatial summation previously observed in wide-field motion-sensitive neurons in *M. stellatarum* (*16*), we compared the spatial summation predictions extracted from the responses of these neurons with our LMC responses at the same respective light intensities. To this end, we convolved the photoreceptor receptive fields with the average spatial summation that was estimated as a Gaussian low-pass filter (*16*). We then calculated the root mean square deviation (RMSD) between the spatial summation kernel and the individual LMC responses at each light intensity using ANOVA (normality of residuals confirmed) with Bonferroni-corrected post hoc comparisons (Fig. 3D, fig. S5, and table S2). Models with RMSD smaller or equal to the RMSD of physiological responses were deemed good fits.

We compared the responses of the identified and unidentified subsets of LMCs quantitatively by calculating the RMSD between each individual neuron of the two populations and compared it statistically to the RMSD between neurons within populations using ANOVA (normality of residuals confirmed; table S4). We then generated response predictions for type II LMCs from their average dendritic distributions obtained in previous anatomical studies (Fig. 4A) (*5*). These give the number of dendrites of specific lengths (in visual angle) for each LMC type. The data from these distributions were directly used to generate spatial filters to predict the spatial characteristics of the LMC responses. To predict the responses based on all dendrites of type II LMCs (all), we converted the dendrite histogram into a continuous function, which was then mirrored around its origin to obtain a symmetric function of dendrite distributions as a function of visual angle (Fig. 4B). This function was then normalized to 1 and convolved with the normalized photoreceptor angular response profile at each light intensity (Fig. 2B) to produce predictions of the LMCs' responses at the same light intensities (Fig. 4, C and D). This prediction assumes, for simplicity, that LMCs integrate linearly from all their dendrites. In addition, we also generated a model containing only the core dendrites (i.e., those restricted to the home cartridge—short) and one that contained only the long dendrites (i.e., those that project outside the home cartridge—long). To test the goodness of fit of these response predictions with the responses of the LMCs measured physiologically, we calculated the RMSD between the model at a given light intensity and each individual recorded LMC response at that intensity (Fig. 4, E and F). We compared the RMSD values of each model prediction to the RMSD values of the physiological responses using ANOVA (normality of residuals confirmed) with Bonferroni-corrected post hoc comparisons (table S3). We deemed models with RMSD below or equal to that of the LMC population good fits, while those with significantly larger RMSD were considered poor fits.

SUPPLEMENTARY MATERIALS

Supplementary material for this article is available at http://advances.sciencemag.org/cgi/content/full/6/16/eaaz8645/DC1

REFERENCES AND NOTES

1. J. A. De Carlos, J. Borrell, A historical reflection of the contributions of Cajal and Golgi to the foundations of neuroscience. *Brain Res. Rev.* **55**, 8–16 (2007).
2. S. R. Cajal, D. Sánchez, Contribución al conocimiento de los centros nerviosos de los insectos. *Trab. Lab. Inv. Biol.* **13**, 1–68 (1915).
3. B. Greiner, W. A. Ribi, W. T. Wcislo, E. J. Warrant, Neural organisation in the first optic ganglion of the nocturnal bee *Megalopta genalis*. *Cell Tissue Res.* **318**, 429–437 (2004).
4. B. Greiner, W. A. Ribi, E. J. Warrant, A neural network to improve dim-light vision? Dendritic fields of first-order interneurons in the nocturnal bee *Megalopta genalis*. *Cell Tissue Res.* **322**, 313–320 (2005).
5. A. L. Stöckl, W. A. Ribi, E. J. Warrant, Adaptations for nocturnal and diurnal vision in the hawkmoth lamina. *J. Comp. Neurol.* **524**, 160–175 (2016).
6. N. J. Strausfeld, *Arthropod Brains: Evolution, Functional Elegance, and Historical Significance* (Harvard Univ. Press, 2012).
7. N. J. Strausfeld, A. D. Blest, The optic lobes of Lepidoptera. *Philos. Trans. R. Soc. Lond. B Biol. Sci.* **258**, 81–134 (1970).
8. E. J. Warrant, Seeing better at night: Life style, eye design and the optimum strategy of spatial and temporal summation. *Vision Res.* **39**, 1611–1630 (1999).
9. A. Dubs, The spatial integration of signals in the retina and lamina of the fly compound eye under different conditions of luminance. *J. Comp. Physiol.* **146**, 321–343 (1982).
10. A. Dubs, S. B. Laughlin, M. V. Srinivasan, Single photon signals in fly photoreceptors and first order interneurones at behavioral threshold. *J. Physiol.* **317**, 317–334 (1981).
11. J. H. van Hateren, Theoretical predictions of spatiotemporal receptive fields of fly LMCs, and experimental validation. *J. Comp. Physiol. A* **171**, 157–170 (1992).
12. K.-F. Fischbach, A. P. M. Dittrich, The optic lobe of *Drosophila melanogaster*. I. A Golgi analysis of wild-type structure. *Cell Tissue Res.* **258**, 441–475 (1989).
13. N. J. Strausfeld, The optic lobes of Diptera. *Philos. Trans. R. Soc. Lond. B Biol. Sci.* **258**, 135–223 (1970).
14. V. Braitenberg, Patterns of projection in the visual system of the fly. I. Retina-lamina projections. *Exp. Brain Res.* **3**, 271–298 (1967).
15. K. Kirschfeld, The projection of the optical environment on the screen of the rhabdomere in the compound eye of the *Musca*. *Exp. Brain Res.* **3**, 248–270 (1967).
16. A. L. Stöckl, D. C. O'Carroll, E. Warrant, Higher-order neural processing tunes motion neurons to visual ecology in three species of hawkmoths. *Proc. Biol. Sci.* **284**, 20170880 (2017).
17. A. L. Stöckl, D. C. O'Carroll, E. J. Warrant, Neural summation in the hawkmoth visual system extends the limits of vision in dim light. *Curr. Biol.* **26**, 821–826 (2016).
18. A. Borst, Fly visual course control: Behaviour, algorithms and circuits. *Nat. Rev. Neurosci.* **15**, 590–599 (2014).
19. S.-y. Takemura, A. Nern, D. B. Chklovskii, L. K. Scheffer, G. M. Rubin, I. A. Meinertzhagen, The comprehensive connectome of a neural substrate for 'ON' motion detection in *Drosophila*. *eLife* **6**, e24394 (2017).
20. K. Shinomiya, G. Huang, Z. Lu, T. Parag, C. S. Xu, R. Aniceto, N. Ansari, N. Cheatham, S. Lauchie, E. Neace, O. Ogundeyi, C. Ordish, D. Peel, A. Shinomiya, C. Smith, S. Takemura, I. Talebi, P. K. Rivlin, A. Nern, L. K. Scheffer, S. M. Plaza, I. A. Meinertzhagen, Comparisons between the on- and off-edge motion pathways in the *Drosophila* brain. *eLife* **8**, e40025 (2019).
21. M. Rivera-Alba, S. N. Vitaladevuni, Y. Mishchenko, Z. Lu, S.-y. Takemura, L. Scheffer, I. A. Meinertzhagen, D. B. Chklovskii, G. G. de Polavieja, Wiring economy and volume exclusion determine neuronal placement in the *Drosophila* brain. *Curr. Biol.* **21**, 2000–2005 (2011).
22. S.-y. Takemura, A. Bharioke, Z. Lu, A. Nern, S. Vitaladevuni, P. K. Rivlin, W. T. Katz, D. J. Olbris, S. M. Plaza, P. Winston, T. Zhao, J. A. Horne, R. D. Fetter, S. Takemura, K. Blazek, L.-A. Chang, O. Ogundeyi, M. A. Saunders, V. Shapiro, C. Sigmund, G. M. Rubin, L. K. Scheffer, I. A. Meinertzhagen, D. B. Chklovskii, A visual motion detection circuit suggested by *Drosophila* connectomics. *Nature* **500**, 175–181 (2013).
23. S. Y. Takemura, C. S. Xu, Z. Lu, P. K. Rivlin, T. Parag, D. J. Olbris, S. Plaza, T. Zhao, W. T. Katz, L. Umayam, C. Weaver, H. F. Hess, J. A. Horne, J. Nunez-Iglesias, R. Aniceto, L.-A. Chang, S. Lauchie, A. Nasca, O. Ogundeyi, C. Sigmund, S. Takemura, J. Tran, C. Langille, K. Le Lacheur, S. McLin, A. Shinomiya, D. B. Chklovskii, I. A. Meinertzhagen, L. K. Scheffer, Synaptic circuits and their variations within different columns in the visual system of *Drosophila*. *Proc. Natl. Acad. Sci. U.S.A.* **112**, 13711–13716 (2015).
24. J. C. Tuthill, A. Nern, S. L. Holtz, G. M. Rubin, M. B. Reiser, Contributions of the 12 neuron classes in the fly lamina to motion vision. *Neuron* **79**, 128–140 (2013).
25. W. A. Ribi, Anatomical identification of spectral receptor types in the retina and lamina of the Australian orchard butterfly, *Papilio aegeus aegeus* D. *Cell Tissue Res.* **247**, 393–407 (1987).

26. J. Rusanen, M. Weckström, Frequency-selective transmission of graded signals in large monopolar neurons of blowfly *Calliphora vicina* compound eye. *J. Neurophysiol.* **115**, 2052–2064 (2016).
27. J. Rusanen, R. Frolov, M. Weckström, M. Kinoshita, K. Arikawa, Non-linear amplification of graded voltage signals in the first-order visual interneurons of the butterfly *Papilio xuthus*. *J Exp Biol* **221**, jeb179085 (2018).
28. M. Joesch, B. Schnell, S. V. Raghu, D. F. Reiff, A. Borst, On and Off pathways in *Drosophila* motion vision. *Nature* **468**, 300–304 (2010).
29. J. Rusanen, A. Vähäkainu, M. Weckström, K. Arikawa, Characterization of the first-order visual interneurons in the visual system of the bumblebee (*Bombus terrestris*). *J. Comp. Physiol. A* **203**, 903–913 (2017).
30. J. H. van Hateren, A theory of maximizing sensory information. *Biol. Cybern.* **68**, 23–29 (1992).
31. Y. E. Fisher, J. C. S. Leong, K. Sporar, M. D. Ketkar, D. M. Gohl, T. R. Clandinin, M. Silies, A class of visual neurons with wide-field properties is required for local motion detection. *Curr. Biol.* **25**, 3178–3189 (2015).
32. J. Schindelin, I. Arganda-Carreras, E. Frise, V. Kaynig, M. Longair, T. Pietzsch, S. Preibisch, C. Rueden, S. Saalfeld, B. Schmid, J.-Y. Tinevez, D. J. White, V. Hartenstein, K. Eliceiri, P. Tomancak, A. Cardona, Fiji: An open-source platform for biological-image analysis. *Nat. Methods* **9**, 676–682 (2012).
33. D. C. O'Carroll, S. D. Wiederman, Contrast sensitivity and the detection of moving patterns and features. *Philos. Trans. R. Soc. Lond. B Biol. Sci.* **369**, 20130043 (2014).
34. E. Rigosi, S. D. Wiederman, D. C. O'Carroll, Visual acuity of the honey bee retina and the limits for feature detection. *Sci. Rep.* **7**, 45972 (2017).

Acknowledgments: We would like to thank the Wiederman laboratory at Adelaide University for sharing their data acquisition and stimulation software. **Funding:** This research was supported by the Swedish Research Council (VR 621-2012-2205), the Knut and Alice Wallenberg Foundation, the Australian Research Council's Discovery Projects funding scheme (project number DP130104561), and the Swedish Foundation for International Cooperation in Research and Higher Education (STINT 2012-2033). **Author contributions:** Conceptualization: A.L.S., E.J.W., and D.C.O. Methodology: A.L.S., D.C.O., and E.J.W. Investigation: A.L.S. Formal analysis: A.L.S. Writing (original draft): A.L.S. Writing (review and editing): A.L.S., D.C.O., and E.J.W. Visualization: A.L.S. Funding acquisition: E.J.W. and D.C.O. Resources: E.J.W. and D.C.O. **Competing interests:** The authors declare that they have no competing interests. **Data and materials availability:** All data needed to evaluate the conclusions in the paper are present in the paper and/or the Supplementary Materials. Additional data related to this paper may be requested from the authors.

Submitted 15 October 2019
Accepted 23 January 2020
Published 17 April 2020
10.1126/sciadv.aaz8645

Citation: A. L. Stöckl, D. C. O'Carroll, E. J. Warrant, Hawkmoth lamina monopolar cells act as dynamic spatial filters to optimize vision at different light levels. *Sci. Adv.* **6**, eaaz8645 (2020).